Behavior Reveals Selective Summation and Max Pooling among Olfactory Processing Channels

Highlights

- Optogenetic fictive odors attract *Drosophila* only when paired with wind

- Single olfactory receptor neuron (ORN) types can produce attraction or repulsion

- Some pairs of ORN types have behavioral effects that sum linearly

- Other pairs yield a behavioral response equal to the larger component (max pooling)

Authors

Joseph S. Bell, Rachel I. Wilson

Correspondence

rachel_wilson@hms.harvard.edu

In Brief

Bell and Wilson show that optogenetic fictive odors, when paired with wind, can attract or repel *Drosophila*. When specific pairs of glomeruli are stimulated simultaneously, their behavioral effects can sum linearly or nonlinearly, depending on the identity of both glomeruli.

CrossMark

CellPress

Article

Behavior Reveals Selective Summation and Max Pooling among Olfactory Processing Channels

Joseph S. Bell[1] and Rachel I. Wilson[1,*]
[1]Department of Neurobiology, Harvard Medical School, Boston, MA 02115, USA
*Correspondence: rachel_wilson@hms.harvard.edu
http://dx.doi.org/10.1016/j.neuron.2016.06.011

SUMMARY

The olfactory system is divided into processing channels (glomeruli), each receiving input from a different type of olfactory receptor neuron (ORN). Here we investigated how glomeruli combine to control behavior in freely walking *Drosophila*. We found that optogenetically activating single ORN types typically produced attraction, although some ORN types produced repulsion. Attraction consisted largely of a behavioral program with the following rules: at fictive odor onset, flies walked upwind, and at fictive odor offset, they reversed. When certain pairs of attractive ORN types were co-activated, the level of the behavioral response resembled the sum of the component responses. However, other pairs of attractive ORN types produced a response resembling the larger component (max pooling). Although activation of different ORN combinations produced different levels of behavior, the rules of the behavioral program were consistent. Our results illustrate a general method for inferring how groups of neurons work together to modulate behavioral programs.

INTRODUCTION

The relationship between neural activity and behavior has been studied most extensively for single neurons (Parker and Newsome, 1998). However, information is generally represented not by single neurons, but by populations of neurons. Neural populations can often be divided into groups based on selectivity or function. Ideally, we would like to infer how groups of neurons work together to modulate behavior, but this inference requires independent control of the different groups. Recently, new genetic techniques have made it possible to control cell classes within a neural population.

The olfactory system is particularly amenable to genetic approaches to understanding the relationship between neural activity and behavior. This is because each olfactory processing channel, or glomerulus, is associated with a unique gene. This gene is the odorant receptor expressed by all the olfactory receptor neurons (ORNs) that project to that glomerulus (Su et al., 2009). A genetic approach is particularly tractable in *Drosophila*, where the number of ORN types (∼50) is relatively small, and almost every one has been matched with its cognate receptor (Couto et al., 2005; Fishilevich and Vosshall, 2005; Silbering et al., 2011). A typical odor activates multiple ORN types, so many olfactory behaviors are thought to be driven by several ORN types working together (Su et al., 2009).

Previous studies in *Drosophila* have mainly used two approaches to infer the contributions of different ORN types to behavior. The first is to measure both ORN activity and behavior evoked by many odors. Linear regression is then used to infer the specific contribution, or "weight," of each ORN type. These studies found positive and negative weights associated with specific ORN types (Knaden et al., 2012; Kreher et al., 2008). However, a limitation of these approaches is that the odor responses of different ORN types are statistically correlated (Haddad et al., 2010): an odor stimulus that strongly activates a given receptor tends to strongly activate other receptors as well. Because multiple ORN types are often co-activated by attractive odors, linear regression cannot tell us which ORN type causes the attraction.

A second approach is to silence a specific ORN type and measure the resulting change in behavior (Kurtovic et al., 2007; Semmelhack and Wang, 2009; Stensmyr et al., 2012; Suh et al., 2004). Studies using this approach have identified several instances in which silencing an ORN type reduces or abolishes a behavioral response to a specific odor. Studies in mammals have obtained similar results (Dewan et al., 2013; Keller et al., 2007). However, a behavior could depend on co-activation of several ORN types and might be abolished by silencing any one of them. Necessity only implies sufficiency if the behavior depends on a single ORN type in a manner that is independent of other ORN types.

In short, the interpretation of previous studies hinges on a key question. Does each ORN type have an influence on behavior that is independent of the influence of other ORN types? In other words, do signals from different ORN types combine linearly?

Here we directly investigate this question by using optogenetic tools that allow us to activate specific ORN types (Bellmann et al., 2010; Hernandez-Nunez et al., 2015; Suh et al., 2007). Our study can be divided into three parts. In part 1, we demonstrate that freely walking flies exhibit a robust behavioral response to optogenetic fictive odors when these stimuli are paired with air currents. We describe the elements of this

A
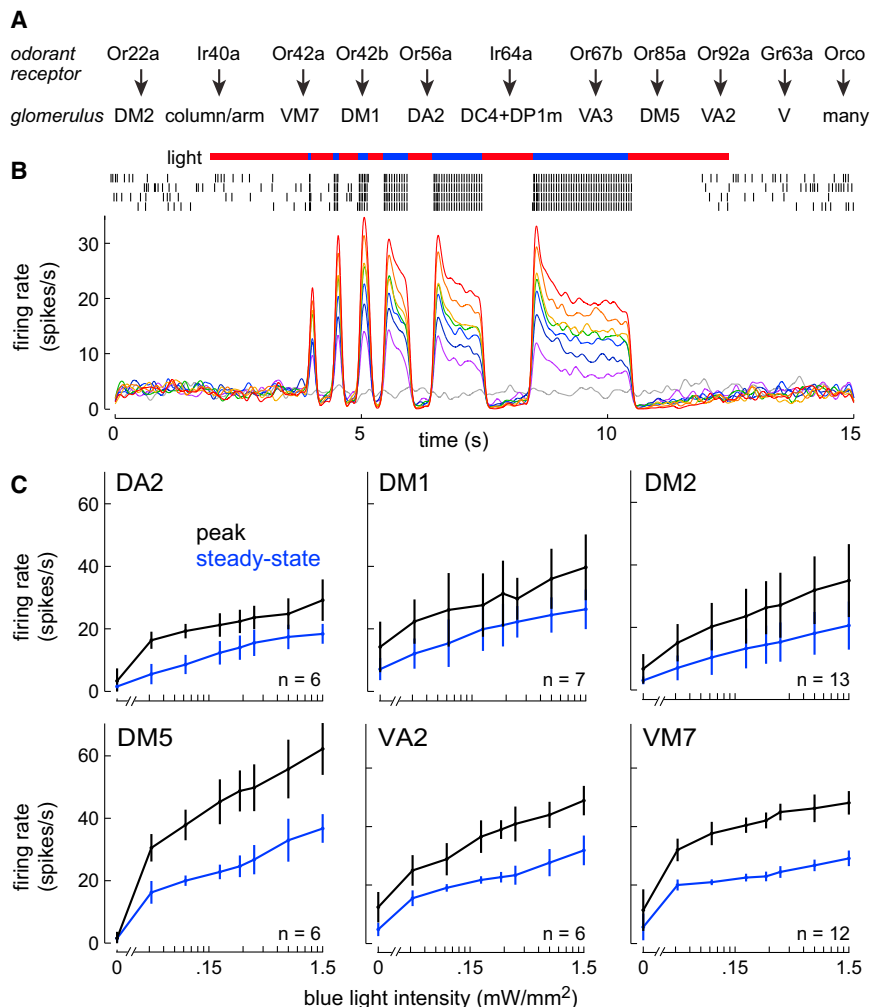
Figure 1. Graded Optogenetic Recruitment of Specific ORN Types

(A) Odorant receptors expressed by the ORN types in this study, and their cognate glomeruli. Ir40a is expressed by ORNs targeting two glomeruli, and the same is true of Ir64a. Orco is a co-receptor that is expressed in most ORNs. Receptor expression data are from Couto et al. (2005), Fishilevich and Vosshall (2005), Larsson et al. (2004), Ai et al. (2010), and Silbering et al. (2011).

(B) Example spike raster from a ChR+ ORN projecting to glomerulus DM2; note the high trial-to-trial reliability. Red and blue bars signify red and blue light (here both 1.5 mW/mm^2). Below are peri-stimulus time histograms averaged across all DM2 ORN recordings (n = 13 ORNs) for a variety of blue light intensities. Warmer colors indicate increasing blue light intensity (gray = 0, red = maximum, i.e., 1.5 mW/mm^2). In cases where blue light was delivered at an intensity less than the maximum, we simultaneously illuminated the antenna with a compensatory amount of red light. Blue light was presented for a variety of durations, because a fly in the behavior chamber also experiences a variety of durations. Firing rate dynamics were similar in all ORN types (Figure S1).

(C) Light-evoked firing rates in ChR+ ORNs (mean ± SD across cells). Steady-state firing rates were measured over 2 s of continuous blue light illumination, i.e., the longest blue pulse in (B). Peak firing rates were measured over a 100 ms pulse (in the stimulus train, this is the third blue bar from the left). Both peak firing rate and steady-state firing rate decreased log-linearly as blue light intensity decreased. Note that the maximal evoked firing rate was similar in most of these ORN types. We report steady-state ORN firing rates in the rest of the study. See Table S1 for all genotypes.

behavior, and we define a simple metric for the frequency of observing this behavior (the overall "level" of behavior). In part 2, we compare the level of behavior driven by individual ORN types and their pairwise combinations. The main finding of the study is that signals from certain pairs of attractive ORN types sum roughly linearly, whereas other pairs combine nonlinearly via max pooling. In essence, each attractive ORN type produces a variable incremental effect on the level of behavior, depending on what other ORN type was co-activated. These dependencies may relate to whether ORN types provide redundant cues about the value of an odor. Finally, in part 3, we confirm that we are observing essentially the same behavioral program in all genotypes, meaning that the elements of the behavioral response are similar across genotypes, and different genotypes differ mainly in the overall level of their response.
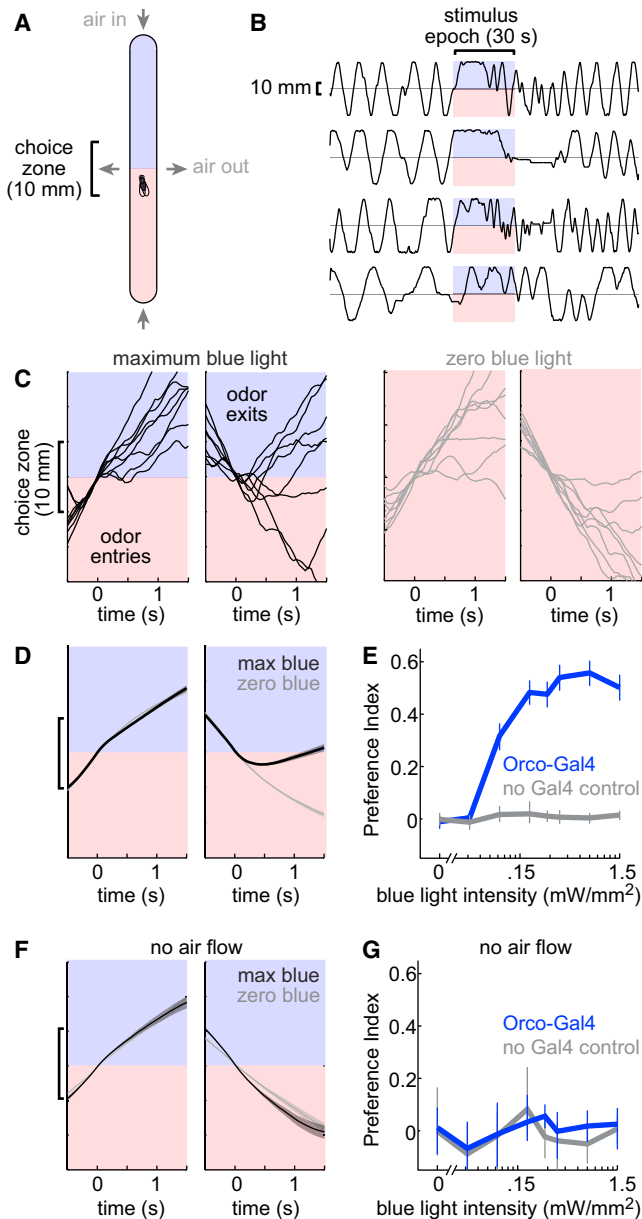
RESULTS

Controlling Olfactory Receptor Neurons with Light

We expressed the light-gated ion channel *channelrhodopsin-2* (ChR) in multiple individual ORN types under the control of the Gal4/UAS system (Figure 1A; Tables S1 and S2). To evoke

ORN spikes, we illuminated the antenna with blue light. To minimize thermal fluctuations (which will become important for behavioral tests, see below), we added a red laser to the stimulus protocol. During the stimulus epoch, pulses of blue light were interleaved with red light, so that total intensity (blue+red) was held constant (at 1.5 mW/mm^2).

As expected, blue light increased spike rates in ChR-expressing ORNs (Figure 1B). The red light lies outside the excitation spectrum of ChR, and indeed red light did not increase ORN firing rates. When we repeated these experiments with several different ORN types, we found that the magnitude and the dynamics of light-evoked responses were similar in most cases (Figure S1).

When we decreased blue light intensity, ORN firing rates decreased log-linearly (Figure 1C; here we co-illuminated with red and blue light to always keep total intensity constant at 1.5 mW/mm^2). The dynamic range of ORN firing rates that we could achieve was constrained by the need to avoid off-target behavioral effects of light (see below). However, it should be noted that real odors elicit firing rates in this same range (Hallem and Carlson, 2006), and as we will show, these firing rates are capable of eliciting significant behavioral responses. Henceforth,

we will sometimes refer to our stimuli as activating "glomeruli." This is a convenient shorthand, but it should be kept in mind that we are driving the ORN input to a glomerulus, not the glomerulus proper.

Behavioral Attraction Emerges from Simple Rules

To measure olfactory behavior, we placed individual blind flies (hemizygous males harboring the *NorpA7* mutation) in narrow plastic chambers. Air flowed into both ends of each chamber and flowed out through ports at the mid-point (Figure 2A). Flies tend to pace back and forth along these chambers (Figure 2B), as shown previously (Claridge-Chang et al., 2009; Parnas et al., 2013).

During the stimulus epoch, flies were illuminated with blue light in only one half of the chamber (the "odorized" half). In the other half of the chamber, flies were illuminated with red light (1.5 mW/mm²) in order to minimize temperature differences between the two halves (Figure S2). We used eight blue light intensities in each experiment, ranging from 0 to 1.5 mW/mm². When the blue light intensity was less than 1.5 mW/mm², we added a compensatory amount of red light to the "odorized" half of the chamber, so that total light intensity was constant at all locations during the stimulus epoch, and across epochs with different blue light intensities. We repeated each blue light intensity 16 times in each experiment, resulting in a total of 5.3 hr of observation for each fly. In this study as a whole, we tracked over 2,600 flies for a total of more than 14,000 hr of observation.

We began by expressing ChR under the control of *Orco-Gal4* (Larsson et al., 2004) in order to stimulate the majority of ORNs. To understand how flies are responding to this stimulus, we inspected the walking trajectories of individual flies around the time that they entered or exited the fictive odor (Figures 2C and 2D). Following entry, flies continued walking normally. But following exit, flies reversed more than usual and re-entered the fictive odor.

We quantified behavior by counting the fly's exits from a choice zone at the mid-point of the chamber (Figure 2A, following Claridge-Chang et al., 2009; Parnas et al., 2013). Choices were used to compute a Preference Index (PI), where +1 indicates the fly always chooses the "odorized" side, and −1 indicates the fly always chooses the "non-odorized" side. PI is highly correlated with occupancy on the "odorized" side (R = 0.95). PI in these flies increased with light intensity and peaked close to 0.6, indicating a robust preference for the fictive odor

Figure 2. A High-Throughput Assay for Measuring Behavioral Responses to Optogenetic Fictive Odors

(A) Behavioral chamber. Air flowed in at the ends and out through vents at the midpoint. A fly encountered blue light in one half of the chamber. In the other half, the fly was illuminated with red light (always 1.5 mW/mm²). In trials where the blue light intensity was less than maximum (i.e., <1.5 mW/mm²), red light was added to the blue zone so that total intensity at all locations in all trials was 1.5 mW/mm².

(B) Example trajectories of four flies. Each trajectory shows one fly's position along the long axis of the chamber over time. Flies express ChR in most ORNs (under *Orco-Gal4* control).

(C) Trajectories aligned to when the fly crossed the chamber's midpoint (time = 0), grouped by heading direction at that point. Flies express ChR under *Orco-Gal4* control. Black: maximum blue light intensity (1.5 mW/mm²). Gray: zero blue light intensity. Note that exiting the fictive odor tends to produce abrupt reversal, while entering the fictive odor has little effect.

(D) Same as (C) but averaged across all trajectories from all flies of this genotype. Mean trajectories are overlaid for maximum-blue and zero-blue trials. Shaded bands represent SEM across flies (n = 72 flies).

(E) Mean PI versus blue light intensity (±bootstrapped 95% confidence intervals). In flies expressing ChR under *Orco-Gal4* control, PI increases with light intensity. In control flies that lack Gal4, blue light does not affect PI (n = 72 flies for *Orco-Gal4*, 64 for no Gal4). The two genotypes are significantly different (p < 0.0001, see Supplemental Experimental Procedures for statistical test).

(F and G) Same as (D) and (E) but for experiments where air flow was turned off (n = 32 flies for *Orco-Gal4*, 24 for no Gal4). Here there is no preference. There is no statistical difference between the two genotypes in the relationship between PI and blue light intensity (p = 0.86).
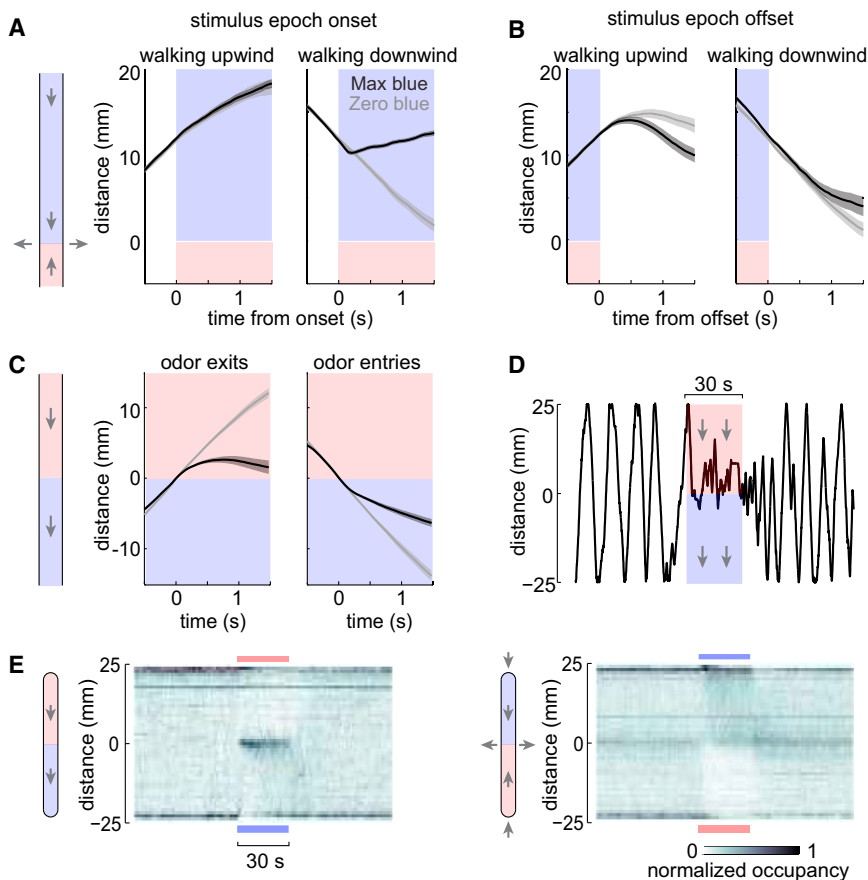
Figure 3. Fictive Odor Onset Causes Upwind Turns, and Offset Causes Downwind Turns

(A) Mean trajectories aligned to the onset of the stimulus epoch, ±SEM across flies (n = 72 flies). We included all the trajectories where, at stimulus epoch onset, the fly was positioned 8–16 mm from the blue end of the chamber. Left: flies walking upwind at fictive odor onset showed little deviation from the zero-blue laser controls. Right: flies walking downwind at fictive odor onset tended to reverse and walk upwind more often than the zero-blue laser controls. We assessed statistical significance by measuring position over the last half-second of these trajectories; position was not significantly different on the left (p = 0.90) but was highly significant on the right (p < 0.0005). In all panels of this figure, flies express ChR under *Orco-Gal4* control.

(B) Same as (A), but aligned to the end of each stimulus epoch. Flies walking upwind tended to reverse and walk back downwind more often than did zero-blue laser controls (p = 0.03). For flies walking downwind, there is no significant difference from the zero-blue laser controls (p = 0.46). The four p values associated with this figure were corrected for multiple comparisons using the Bonferroni-Holm procedure (m = 4 tests).

(C) Rather than flowing air into the chamber at both ends and out at the mid-point (as in all other experiments), we instead flowed air in one direction through the entire chamber. The fictive odor was placed on the downwind side. Mean trajectories aligned to fictive odor entry or exit show that flies tended to turn after downwind entries and also after upwind exits (n = 32 flies, ±SEM across flies).

(D) Example single-fly trajectory from an experiment like that in (C). Arrows show air flow direction. Note that the fly repeatedly re-crosses the fictive odor boundary.

(E) Histograms of occupancy over time, averaged over all flies tested in each condition. Left: in the modified chamber with one-way air flow, flies reverse in response to blue light entry and also blue light exit, causing them to remain mostly in the mid-point of the chamber. Right: in the standard chamber with air flowing in at both ends, flies accumulate on the side with the fictive odor.

(Figure 2E). Flies that lacked ChR expression in ORNs showed no attraction (Figure 2E).

A previous study found no behavioral effect of stimulating *Orco+* ORNs optogenetically (Suh et al., 2007), and so we wondered whether a key difference might be the absence of airflow in the previous study. Indeed, when we stopped airflow through the chamber, flies were no longer attracted to the fictive odor (Figures 2F and 2G).

What are the contributions of olfactory cues and airflow cues to this behavior? To address this, we examined the start and end of the stimulus epoch. These are the time points when the fictive odor is turned on or off without regard to the fly's position. At these time points, the change in the fictive odor can occur when the fly is facing either upwind or downwind.

We found that the effect of fictive odor depended on wind direction. Fictive odor onset caused the fly to reverse when it was facing downwind, but it had little effect when the fly was already facing upwind (Figure 3A). This makes sense: real odors are carried downwind from their sources, and so moving upwind is an effective strategy for locating an odor source.

Conversely, when the fly lost the fictive odor while heading upwind, it tended to reverse (Figure 3B). This also makes sense: in a natural setting, if the fly loses contact with an odor plume, a reversal may allow the fly to relocate the plume. There was also a non-significant trend for flies to reverse after losing the fictive odor while heading downwind.

These results imply two rules: (1) walk upwind at odor onset, and (2) reverse at odor offset (especially if heading upwind at odor offset). To test whether these rules generalize to a different context, we flowed air in one direction through the entire chamber, and we placed the fictive odor on the downwind side. The result was striking: flies tended to reverse after encountering the fictive odor, and also to reverse after leaving it (Figure 3C). The result is that they often simply circled back and forth across the fictive odor boundary (Figures 3D and 3E). Reversing after a fictive odor encounter is clear evidence that a fly is not following the direction of odor intensity changes. Instead, it is following wind cues—it is turning upwind in response to the fictive odor, even though this causes it to move out of the odorized half of the chamber. This paradoxical

A

B

C
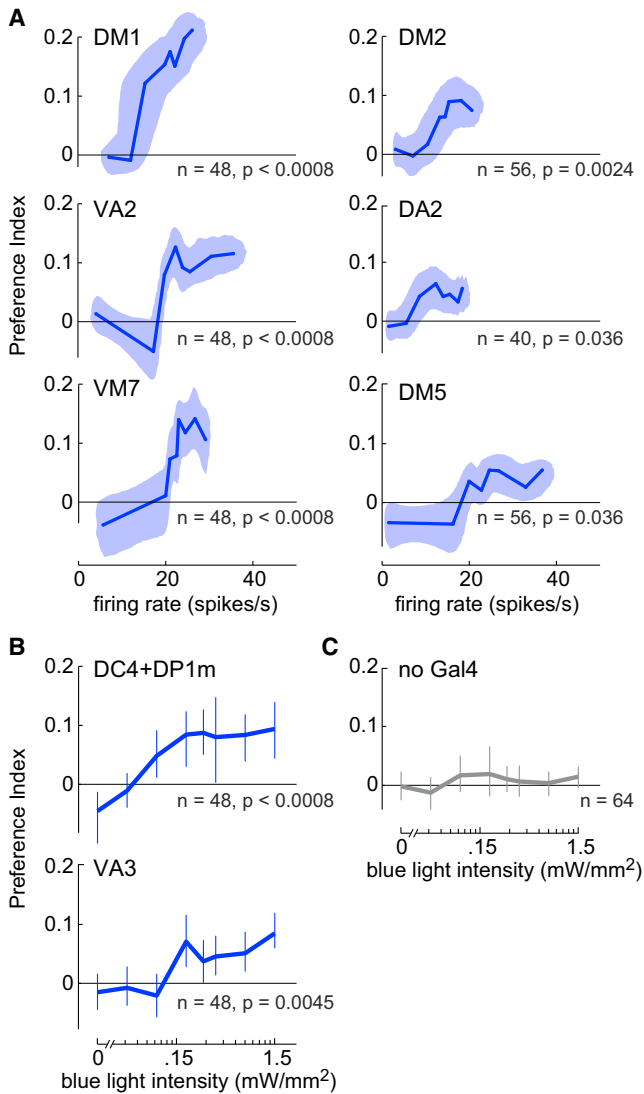
Figure 4. Attraction Evoked by Individual ORN Types

(A) Mean PI versus ORN spike rate, for the six "attractive" ORN types we were able to record from (firing rate data are the steady-state firing rates from Figure 1C). Shaded bands show bootstrapped 95% bivariate confidence intervals. p values represent comparisons with control flies that do not express ChR ("no Gal4" control), after correction for multiple comparisons using the Bonferroni-Holm procedure (m = 8 tests, see Supplemental Experimental Procedures).

(B) Mean PI (±bootstrapped 95% confidence intervals) versus blue light intensity. Included here are data for the two ORN types that we were not able to record from.

(C) Same as (B) for control flies (no Gal4). Data are reproduced from Figure 2E.

behavior follows directly from Rule 1. Rule 2 causes the fly to circle back: after it leaves the fictive odor, it turns downwind again and so repeats the cycle.

In our standard experimental chambers (Figure 2A), Rule 1 causes the fly to continue walking upwind after entering the fictive odor, and Rule 2 causes it to reverse after exiting the fictive odor. In a later section, we will revisit the question of

what other behaviors, if any, might be latent in our data. For now, we turn to focus on the central question motivating our experiments: what is relationship between neural activity and behavior?

Behavior Evoked by Individual ORN Types

We began by investigating behavioral responses to eight different ORN types. Activating each of these eight ORN types individually produced small but significant attraction (Figures 4A–4C). (Two additional ORN types produced repulsion; see below.) Notably, the threshold for attraction generally corresponded to mean ORN firing rates in the range of 10–20 Hz (Figure 4A).

For every ORN type, increasing stimulus intensity produced increasingly stronger attraction. For some ORN types, this attraction ultimately saturated. This result implies that there are mechanisms downstream of ORN spiking that limit the behavioral effects of single glomeruli.

The saturating level of behavior was not the same for all ORN types; in particular, the DM1 ORNs are able to produce unusually strong behavioral attraction (Figure 4A). This is interesting because previous studies have implicated DM1 as having an especially potent role in triggering attraction (Gao et al., 2015; Semmelhack and Wang, 2009), and the cognate receptor for this glomerulus (Or42b) is the most potently attractive receptor in the entire cohort of larval receptors (Mathew et al., 2013).

In addition to DM1, some of the other ORN types that we identify here as attractive (and/or their cognate odorant receptors) have been associated with attraction in other studies (Table S3). However, several other ORN types that are attractive in our dataset have been previously described as repulsive. In several of these latter cases, some published studies had found repulsion, but others had found attraction (Table S3). These discrepancies between different studies may be due to behavioral context, or the context of other glomeruli co-activated by the odors used in prior studies. Some of these discrepancies may also be due to different evoked ORN firing rates—for example, repulsion might be more prominent if ORN firing rates were higher. Our goal here was not to define the behavioral effect of a given ORN type in all possible contexts. Our goal was to define the effects of multiple individual ORN types within the context of one simple behavioral paradigm, with the ultimate aim of asking how these ORN signals combine to modulate this behavior.

As a control, we asked whether we could replicate our results using alternate Gal4 lines targeting some of the same ORN types. In most cases, the result was the same with the alternate line (Figure S3). In one case, we found a difference, likely because the alternate Gal4 line elicited higher ORN firing rates and so more adaptation; here the difference could be eliminated by reducing ORN firing rates in the alternate line (Figure S4).

It should be noted that the precise relationship between ORN firing and behavior depended on the range of light intensities we used. Lowering all light intensities by 10-fold shifted the relationship to the left (Figure S4). This result is not surprising, given that several studies have described central olfactory adaptation in *Drosophila*, and central adaptation can outlast the stimulus by minutes or longer (Devaud et al., 2001; Sachse et al., 2007).
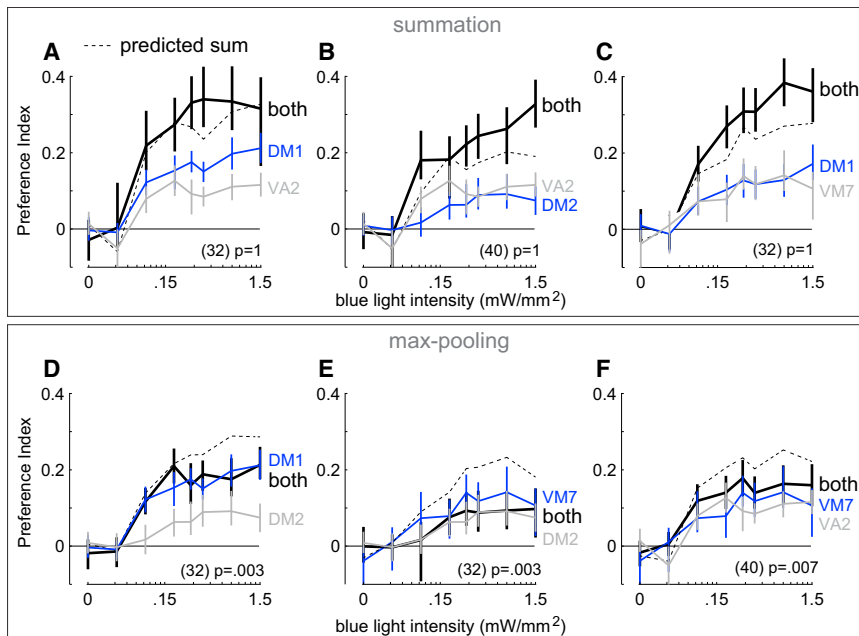
Figure 5. Examples of Summation and Max Pooling among Pairs of ORN Types

(A–C) Examples of summing pairs. Mean PI (±bootstrapped 95% confidence intervals) versus blue light intensity for three combinations of ORN types and their components. The predicted linear sum of each pair of components is shown in dashed lines. For all three pairs, the combination response is similar to (or larger than) the predicted linear sum. Components are reproduced from Figure 4. Values in parentheses are n values for combination data (black). p values represent the probability of responses as small as the data under the null hypothesis of linear summation, after correction for multiple comparisons using the Bonferroni-Holm procedure (see Supplemental Experimental Procedures; m = 28 tests). All three cases are classified as "summation," because the null hypothesis is not rejected. (Note that the DM1 component data are different in (A) and (C) because these data come from two different sets of experiments using distinct Gal4 lines; see Table S1 for genotypes and Figure S3 for comparisons between pairs of alternative Gal4 lines corresponding to the same glomerulus.) (D–F) Examples of max-pooling pairs. Same as above but for the three additional combinations of the same four ORN types. Here the component response is approximately equal to the larger component alone. All three combination responses are significantly smaller than the predicted linear sum. Note that both components of each pair are capable of summing with other ORN types (shown in A–C).

Therefore, we would not expect to find a fixed relationship between ORN firing rates and behavior. It is interesting that, even in the presence of some central adaptation, low ORN firing rates were nonetheless able to elicit behavioral responses.

The Behavioral Effect of a Glomerulus Can Depend on the Identity of Co-active Glomeruli

Next, we investigated the rules of integration by activating pairs of ORN types. If signals from attractive glomeruli are summed linearly, then the response to a pair of glomeruli should equal the sum of the component responses. We would expect to see summation of attraction for every pair of attractive glomeruli in our dataset, because every attractive single glomerulus alone produces a behavioral response that is much less than the maximum observable response (compare Figure 2E and Figure 4).

To examine this prediction, we begin with four attractive glomeruli (DM1, DM2, VA2, and VM7). For some pairs of these glomeruli, we found that their behavioral effects summed roughly linearly. For example, combined stimulation of DM1 and VA2 ORNs produced a response approximately equal to the sum of the two components (Figure 5A). The same was true of DM2 and VA2 (Figure 5B) and also DM1 and VM7 (Figure 5C). These examples show that some pairs of glomeruli do indeed have behavioral effects that sum. Indeed, in all three examples there was a trend for the combination response to exceed the predicted linear sum.

However, some combinations did not sum. For example, pairing DM1 and DM2 produced a response that was significantly smaller than the predicted sum (Figure 5D; see Supplemental Experimental Procedures for statistics). Indeed, the response DM1+DM2 was roughly equal to the larger of the two component re-

sponses alone (DM1). The same was true of VM7 and DM2 (Figure 5E) and also VM7 and VA2 (Figure 5F). In all three cases, the combination response was significantly smaller than the predicted sum and approximately equal to the larger component response. We use the term "max pooling" to describe these cases.
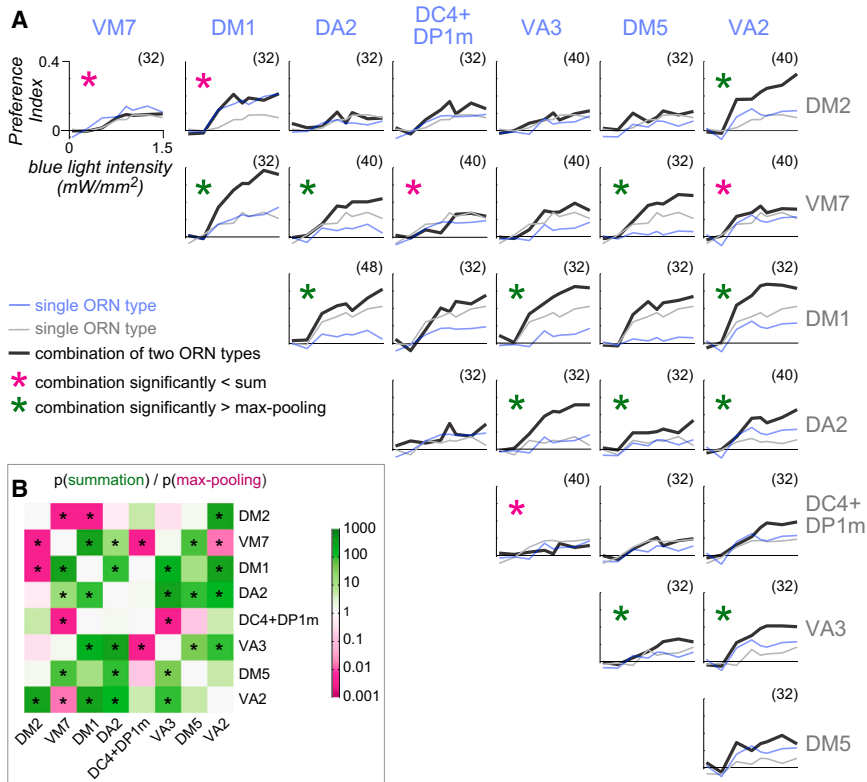
It is worth noting that, in these three latter cases, there was no systematic trend toward summation even at sub-maximal stimulus intensities. Rather, the combination response was usually smaller than the linear prediction across the full range of stimulus intensities. In other words, it did not appear that the two components had been summed and then passed through a saturating nonlinearity that limited only the largest responses.

Together, these examples make two important points. First, the linear model of glomerular integration cannot account for all the data. Second, there appears to be no single rule that governs how channels combine. Some pairs sum approximately linearly, while others are combined sublinearly.

Finally, we asked whether the threshold for stimulus detection is lower in a case where two glomeruli sum. We repeated the experiments with DM1 and VA2 using blue light intensities that were 10-fold weaker, to better sample the near-threshold regime. We found that combining these ORN types did not significantly lower the behavioral response threshold (Figure S5).

Systematically Mapping Interactions between Attractive Glomeruli

To extend this examination to a larger group of olfactory processing channels, we tested all pairwise combinations of the eight attractive glomeruli from Figure 4 and found many examples of either summation or non-summation (Figure 6A). As before, we took summation as the null hypothesis, and we designated a pair as non-summing if the combination response was

Figure 6. Behavioral Responses to All Pairwise Combinations of Eight Attractive ORN Types

(A) Mean PI versus blue light intensity for all pairwise combinations of the eight "attractive" ORN types in Figure 4. All axes have the same range (see top left panel). Blue and gray traces: component responses (reproduced from Figure 4 and Figure S3). Black traces: combination responses (n values in parentheses). Confidence intervals are omitted for clarity. Magenta asterisks: combination response significantly smaller than the sum of the components. Green asterisks: combination response significantly greater than the larger component response. For both tests, the threshold for significance was taken as p < 0.05, after correction for multiple comparisons (m = 28 tests; see Supplemental Experimental Procedures). (Note that not all gray traces in the same row are identical, and not all the blue traces in the same column are identical; this is because not all combinations involving a given ORN type use the same Gal4 line, due to the restrictions imposed by the chromosomal location of each transgene; see Table S1 for genotypes and Figure S3 for comparisons between pairs of alternative Gal4 lines corresponding to the same glomerulus.)

(B) Comparing the outcome of hypothesis testing under two alternative assumptions (assuming summation or assuming max pooling). Color represents the ratio of p values for the summation and max-pooling models. Magenta cells represent combinations more likely under max pooling. Green cells represent combinations more likely under summation. Whitish cells represent combinations that are about equally likely under the two models. Asterisks indicate a significant difference from one model.

significantly smaller than the predicted sum (p < 0.05). Five of the 28 combinations were significantly non-summing. In these five cases, we found no evidence of summation even at low stimulus intensities. Notably, in all five cases, the response to the combination was approximately equal to the larger component response, and so we designate all these cases as max pooling. Importantly, no glomerulus participated exclusively in max pooling. Rather, the nature of the combination depended on the identity of both active glomeruli.

We never observed a case in which two attractive glomeruli together produced less attraction than did either glomerulus alone. Thus, although there was no fixed "weight" associated with each glomerulus, there was a fixed "sign." When an attractive glomerulus was added to an ensemble, it always promoted attraction, or else it had an essentially neutral effect.

We have shown that the data are inconsistent with a model in which all glomeruli sum. Moreover, they are also inconsistent with a model in which all glomeruli are max pooled. We can show this by taking max pooling as the null hypothesis and designating a pair as summing if the combination response was significantly greater than the larger component response (p < 0.05). Twelve of the 28 combinations showed significant summation (Figure 6A).

It is useful to compare the p values arising from the two sorts of statistical tests (Figure 6B). In the first case, the p value expresses the probability of the data (or even smaller responses)

under the hypothesis of summation; in the second case, the p value expresses the probability of the data (or larger responses) under the hypothesis of max pooling. For some pairs of glomeruli, the ratio of the two p values is close to unity, meaning that the data are equally likely under the two hypotheses. These correspond to cases in which one glomerulus had very little effect by itself, and so summation and max pooling are hard to distinguish. However, for many pairs of glomeruli, the two p values are quite different, meaning that these pairs are clear cases of either summation or max pooling.

Activation of Repulsive Glomeruli Can Suppress Responses to Attractive Glomeruli

Until this point, we have focused on a core set of eight "attractive" ORN types. However, we also identified two "anti-attractive" ORN types. One of these projects to glomerulus V and expresses the receptor for carbon dioxide (Suh et al., 2004). We found that this ORN type strongly suppressed attraction mediated by the *Orco+* ORNs (Figure 7A).
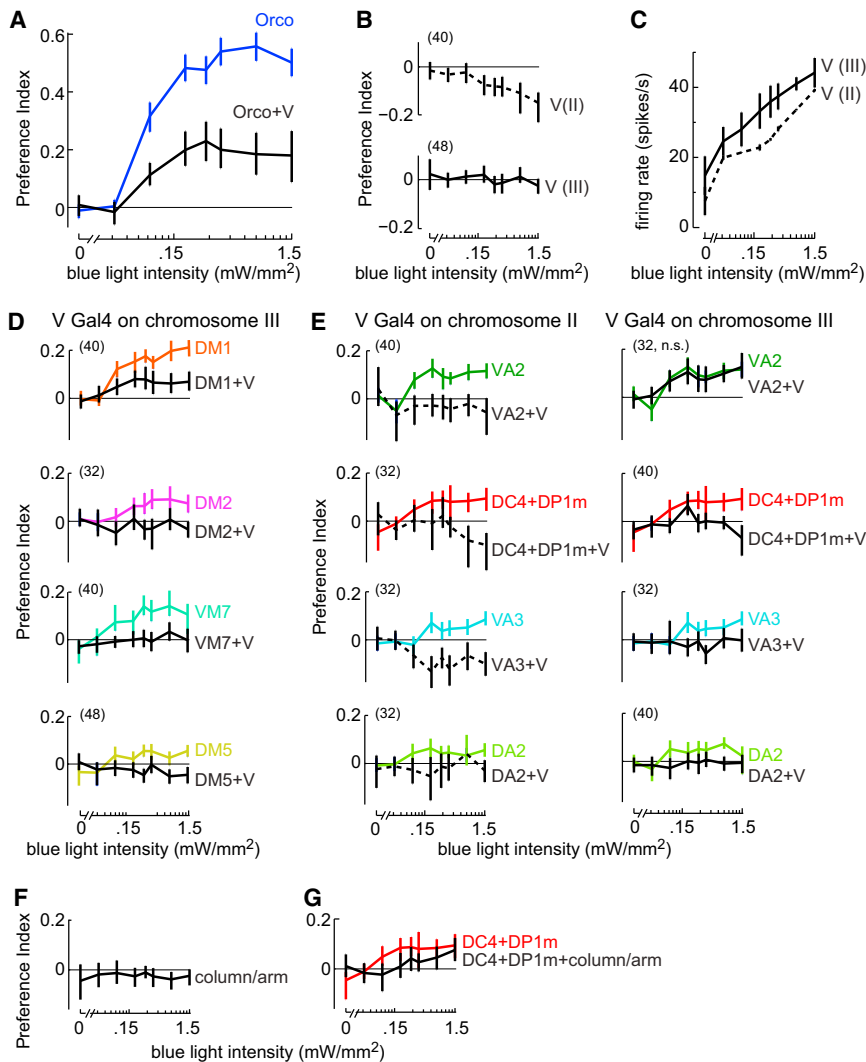
When glomerulus V was activated alone, we observed weak repulsion in one set of experiments, and no behavioral response in a second set of experiments using a different chromosomal insertion of the same Gal4 construct (Figure 7B). The difference between the two Gal4 lines probably relates to differences in ORN firing rates that they evoke (Figure 7C; Figure S3). Previous studies have found a

Figure 7. Activation of Repulsive ORNs Can Suppress Attraction

(A) A potent anti-attractive effect of glomerulus V. Mean PI versus blue light intensity (±bootstrapped 95% confidence intervals). Blue: response to activating most ORNs (under the control of *Orco-Gal4*), reproduced from Figure 2E. Black: activating *Orco*+ ORNs together with V ORNs (n = 32). The combination response is significantly smaller than the response to *Orco*+ ORNs alone (p < 0.0001, see Supplemental Experimental Procedures for statistics). The V Gal4 line used here was the insert on chromosome III (Table S2).

(B) Activating V alone. Mean PI versus blue light intensity (±bootstrapped 95% confidence intervals, n values in parentheses). In experiments using the V Gal4 line on chromosome II (top, dashed line), there is a significant difference (p < 0.001) versus control flies ("no Gal4" control from Figure 2E). In experiments using the V Gal4 line on chromosome III (bottom, solid line), there is no significant difference versus control. Tests are corrected for multiple comparisons (m = 2 tests).

(C) V ORN firing rate versus blue light intensity (mean ± SD across cells, n = 6 and 6 for the Gal4 lines on II and III). Note that both spontaneous and light-evoked firing rates are higher for the Gal4 line on chromosome III, but the behavioral effects for this line are generally weaker, suggesting that there is more central adaptation in this line (Figure S4).

(D and E) Combinations with individual attractive glomeruli. Mean PI versus blue light intensity (±bootstrapped 95% confidence intervals). Colored traces: individual attractive glomeruli, re-plotted from Figure 4. Black: combinations with V (n values in parentheses). All plots have the same axis ranges. The experiments in (D) used the V Gal4 line on chromosome III, and in all cases the effect of the V Gal4 line was statistically significant (p < 0.05). The experiments in (E) used both the V Gal4 line on chromosome II (left, dashed black lines) and the V Gal4 line on chromosome III (right, solid black lines). In all but one case, the effect of V was statistically significant (p < 0.05). In the case of the one exception (VA2 + V Gal4 line on chromosome III, "n.s."), the alternative V Gal4 line showed a significant effect. Tests are corrected for multiple comparisons (m = 12 tests).

(F) Activating column/arm ORNs alone produces small but significant repulsion compared to "no Gal4" control flies (from Figure 2E; p < 0.05; whiskers are bootstrapped 95% confidence intervals, n = 56 for the combination genotype).

(G) Combining column/arm ORNs with DC4+DP1m ORNs significantly reduces behavioral attraction relative to DC4+DP1m alone (from Figure 4B; p < 0.05; whiskers are bootstrapped 95% confidence intervals, n = 32 for the combination genotype).

clear repulsive effect of stimulating glomerulus V in isolation (Faucher et al., 2006; Suh et al., 2004, 2007), which may be due to higher ORN firing rates, or a different behavioral context. In any event, it is interesting that, in our behavioral assay, glomerulus V had a large effect on behavior when combined with *Orco*+ ORNs, although it had a smaller effect when activated alone. This result is further evidence for the conclusion that the behavioral effect of a glomerulus can depend on what other glomeruli are co-activated.

We next tested the effect of combining glomerulus V with each individual attractive glomerulus. In every case, we found a statistically significant suppression of attraction (Figures 7D and 7E). The one exception was when we stimulated VA2 and V together

with one of the V Gal4 constructs, and in this case we obtained a significant effect with the alternative V Gal4 construct (Figure 7E, top row). Together, these results indicate that glomerulus V has widespread anti-attractive effects.

The second anti-attractive ORN type that we identified projects to a glomerulus-like structure called the "column/arm" (Silbering et al., 2011). The odorant receptor expressed by this ORN type may be involved in the behavioral response to the repellent DEET (Kain et al., 2013). We found that the column/arm produced small but statistically significant repulsion when tested alone (Figure 7F). This ORN type also suppressed attraction mediated by other glomeruli (Figure 7G).
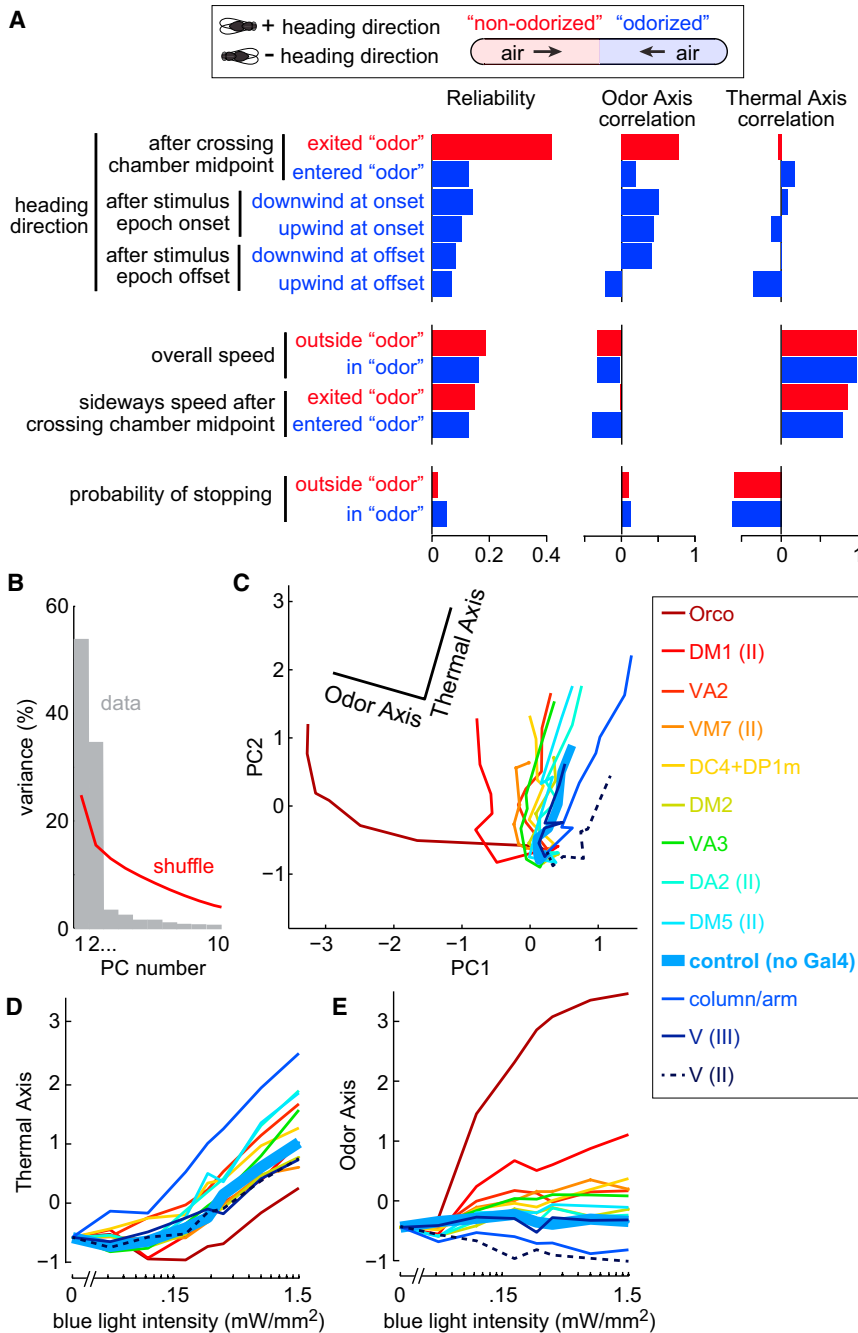
Figure 8. Flies Respond to Fictive Odors with Graded Recruitment of a Single Behavioral Program

(A) Twelve behavioral variables color coded according to whether they are measured inside or outside the "odorized" zone (blue or red). Heading variables are positive when the fly faces the "odorized" end and negative when the fly faces the "non-odorized" end. Heading variables measured after stimulus epoch onset/offset are further divided according to whether the fly was facing upwind or downwind at onset/offset. Shown for each variable is a Reliability score (see Supplemental Experimental Procedures); Reliability = 0 when there is no systematic effect of blue light intensity or genotype, and 1 if the behavior is predictable based on blue light intensity and/or genotype. Reliability is statistically significant for all variables except one (probability of stopping outside "odor"). Also shown is the correlation with the Odor Axis and the Thermal Axis.

(B) Fraction of the explainable variance accounted for by the first 10 principal components (PCs) of this 12-dimensional space. Red line shows the upper 95% confidence interval of the result when PCA is performed after shuffling the genotype and light intensity labels. Only the first two PCs are statistically significant, and together they account for 88% of the variance. Genotypes included are shown in inset at right. Similar results were obtained if *Orco-Gal4* was omitted, or if all combination genotypes were included (see Supplemental Experimental Procedures).

(C) Behavioral data in the space defined by PC1 and PC2. Genotypes cluster at zero intensity and diverge as light intensity increases. Behavior in control flies varies along only one axis in this space (the Thermal Axis). The orthogonal axis (the Odor Axis) accounts for most of the variation that depends on genotype. Genotypes are color coded by PI (Figures 4 and 7). Roman numerals specify the chromosome of the Gal4 line used (Table S2).

(D) Projection of the data onto the Thermal Axis, versus blue light intensity.

(E) Projection of the data onto the Odor Axis, versus blue light intensity.

described component of olfactory navigation in a walking insect, *Drosophila* or otherwise (Kennedy, 1977, 1978). These variables measure the fly's heading direction, speed, and probability of stopping. We measured these variables for all the single-glomerulus genotypes in our dataset, plus the flies in which *Orco-Gal4* drives ChR expression, and the control flies that lack ChR.

We are interested in how blue light modulates these variables. Therefore, we expressed each variable as the change from its baseline value (i.e., its mean value with zero blue light). The baseline level of some variables was genotype dependent (Figure S6), and this should be kept in mind when interpreting our data.

Fictive Odor Evokes a Single Program of Correlated Behaviors

Thus far, we have focused on a single behavioral metric, termed the Preference Index (PI). Does PI capture all the behaviors that are modulated by our fictive odors? In principle, some fictive odors might elicit behaviors that do not affect PI. Also, different detailed behavioral maneuvers could produce the same PI value.

To investigate these questions, we extended our measurements to include a panel of 12 different behavioral variables (Figure 8A; Figure S6). Each of these 12 variables is a previously

First, we asked which behavioral variables are reliably modulated by genotype or blue light intensity, or both. We found that every variable was reliably modulated to a statistically significant degree (Figure 8A), with the exception of one (probability of stopping outside the fictive odor). Thus, many detailed features of behavior are affected by the stimuli in our experiments.

Our goal was not to test whether each behavioral variable is differentially modulated in each genotype, because this would require a larger dataset to obtain meaningful statistical power. Rather, we asked whether all these behaviors are modulated in a coordinated manner—or, alternatively, whether some behaviors are modulated independently of the others. To address this question, we used a linear dimensionality reduction technique, principal component analysis (PCA). Each principal component (PC) represents a linear combination of correlated behavioral changes that result from blue light. If all behaviors are modulated in a coordinated fashion, then we should obtain only one statistically significant PC. Alternatively, if many behaviors can be modulated independently, then we should obtain many significant PCs.

In fact, two PCs were statistically significant (Figure 8B). Together, these two PCs accounted for 88% of the explainable variance in the data. This result means that there are two orthogonal sets of co-modulated behaviors—in other words, two independent behavioral programs.

To better understand these behavioral programs, we projected the intensity-response curves for individual genotypes into the space defined by PC1 and PC2 (Figure 8C). The curve for control flies (which do not express ChR) lay along a straight line in this space, indicating that there is only one behavioral program which is modulated by light in the control flies. The behavioral responses to light in control flies are likely due to thermal cues. Therefore, the axis that captures the control data can be termed the "Thermal Axis" (Figure 8C). The behavior of all genotypes along the Thermal Axis was similar (Figure 8D), suggesting that all genotypes react similarly to temperature cues. The Thermal Axis consisted of speed increases (and stopping decreases) in both halves of the chamber (Figure 8A), implying generalized arousal.

Orthogonal to the Thermal Axis is another axis that captures most of the effects of light that depended on ChR. We term this the "Odor Axis." This behavioral program consisted mainly of heading direction changes at fictive odor onset and offset (Figure 8A). Fictive odor onset caused flies to orient upwind toward the odor end of the chamber. Even more reliably, exits from the "odorized" half of the chamber caused flies to turn around, walk downwind, and return to the fictive odor. Finally, at stimulus epoch offset, flies tended to reverse direction. This description of the Odor Axis is largely consistent with our analyses in Figure 2 and Figure 3. What this broader analysis reveals is that a single behavioral program describes essentially all the effects of fictive odor in our dataset. The frequency of observing this behavioral program increases with blue light intensity, and its peak frequency is highest in the genotypes with the largest PI (Figure 8E; Figure S6). Indeed, the Odor Axis is overall highly correlated with PI (R = 0.71), whereas the Thermal Axis is uncorrelated with PI (R = −0.01).

It is notable that PCA uncovered a nonspecific thermal behavioral program in our dataset (in spite of our best efforts to remove thermal cues), and yet it did not discover any olfactory behavioral program that is uncorrelated with PI. Thus, we can conclude that fictive odor recruited mainly a single behavioral program. This conclusion is further supported by a more extensive analysis we undertook that searched for novel behaviors using a machine learning algorithm (Figure S7). The low dimensionality of olfactory behavior in our data is likely a consequence of the simple experimental paradigm we have used. In other contexts, olfactory behavior may have a higher dimensionality (Jung et al., 2015).

DISCUSSION

Navigation and Olfactory-Mechanosensory Integration

Insects use multiple strategies to navigate toward odor sources (Kennedy, 1977, 1978). One strategy is to turn upwind upon encountering an odor, because odors disperse downwind from the source. Previous studies have shown that *Drosophila* tend to fly or walk upwind in response to odor (Bhandawat et al., 2010; Budick and Dickinson, 2006; Duistermars et al., 2009; Steck et al., 2012; Thoma et al., 2014; van Breugel and Dickinson, 2014). Whereas flying insects must use visual cues to estimate wind direction from their own self-motion, walking insects can use mechanosensory cues to estimate wind direction (Bell and Kramer, 1979).

Here we show that olfactory navigation in walking flies can depend critically on mechanosensory cues. We deduce two rules that account for most of our data: (1) walk upwind in response to odor onset, and (2) reverse at odor offset (especially if heading upwind at odor offset). In a natural setting, these rules should cause the fly to walk toward the odor source, and then backtrack if it overshoots the source or loses the plume.

These rules are similar to those inferred previously from the behavior of freely flying *Drosophila* (Budick and Dickinson, 2006; van Breugel and Dickinson, 2014). Flying flies turn upwind in response to odor onset. When they lose the odor plume, they tend to turn and fly crosswind. Our narrow chambers meant flies had a limited ability to move crosswind, and this may be one reason why they tended to instead turn downwind at odor offset.

Psychophysical Threshold and Saturation

We found that many ORN types could elicit a behavioral response when activated individually. Prior studies in *Drosophila* and mammals have also found that single glomeruli can often drive behavior (Bellmann et al., 2010; Bhandawat et al., 2010; Gaudry et al., 2013; Hernandez-Nunez et al., 2015; Mathew et al., 2013; Smear et al., 2013). Notably, we observed clear behavioral responses to single-glomerulus stimuli that elicited firing rates substantially below 50 spikes/s in each of the active ORNs. This is noteworthy because odors can drive ORNs to fire at rates up to 300 spikes/s, and so responses <50 spikes/s have often been considered to be essentially non-responses (de Bruyne et al., 1999, 2001; Hallem and Carlson, 2006).

We also found that behavioral responses to single ORN types generally saturated at relatively low firing rates. The saturating levels of attraction we observed for single ORN types were much lower than the level evoked by stimulation of many ORN types (using *Orco-Gal4*). What mechanisms might cause

behavioral saturation in response to single-glomerulus stimulation? One possibility is synaptic depression at the synapses made by ORNs onto postsynaptic projection neurons. Depression at these synapses causes postsynaptic responses to saturate as ORN firing rates increase (Kazama and Wilson, 2008). This type of saturation is normally mitigated by lateral inhibition. However, co-activation of multiple glomeruli is generally required to produce lateral inhibition (Olsen et al., 2010), and so our sparse optogenetic stimuli were unlikely to recruit this effect.

Glomerular Combinations: Summation and Max Pooling

The major aim of this study was to understand how signals from different glomeruli combine to influence behavior. Prior to the advent of selective genetic tools, the main approach to this question was to use different odors to activate different groups of glomeruli, and then to ask how the response to an odor mixture compares to the sum of the components alone. Studies using this approach have shown clearly that odor mixtures can elicit behavioral responses that deviate from a linear prediction (Baker, 2008; Jinks and Laing, 2001; Thoma et al., 2014).

Nonetheless, it would be difficult to use odor mixtures to infer how specific glomeruli interact in the brain. Some mixture effects reflect agonistic and antagonistic effects of ligands on odorant receptors (Duchamp-Viret et al., 2003; Turner and Ray, 2009). Moreover, even a monomolecular odor can activate many glomeruli.

Here, we circumvented both these problems by stimulating ORN types optogenetically. We found that some combinations of glomeruli summated roughly linearly, whereas other combinations combined sublinearly. In these latter cases, the rules of glomerular combination appeared to be captured by a max-pooling rule.

If glomerular integration includes a major nonlinear component (as mixture studies have hinted), why have linear models been so successful at fitting behavioral data (Knaden et al., 2012; Kreher et al., 2008)? One reason is that certain combinations of ORN types do sum in a linear manner. Another reason is that each ORN type in our dataset makes a contribution to behavior that has a consistent sign (or valence). Thus, if we simply defined a linear model in which attractive and repulsive channels receive a weight of +1 and −1, respectively, then we would be able to predict a substantial fraction of the behavioral variance in our data. Finally, because the odor responses of different ORN types are correlated (Haddad et al., 2010), predictions of behavior from glomerular activity may be correct by chance, even if the causal roles attributed to certain glomeruli are in fact due to other (correlated) glomeruli.

Circuit Implementation of Summation and Max Pooling

In principle, the computations we have defined on the basis of our behavioral data could be implemented anywhere in the CNS. However, one can begin to find potential implementations in the known elements of the olfactory system. Selective summation among glomeruli might reflect, in part, the convergence of excitatory projections from different glomeruli onto individual neurons in the lateral horn or mushroom body. In the lateral horn, these patterns of convergence are rather stereotyped (Fişek and Wilson, 2014; Jefferis et al., 2007; Tanaka et al., 2004),

whereas in the mushroom body they are more variable (Caron et al., 2013) but still statistically biased (Gruntman and Turner, 2013).

How could max pooling be implemented? Max pooling suggests mutual inhibition, because it implies a comparison between the level of activity in different channels. However, the phenomenon of apparent max pooling does not necessarily imply a mechanism wherein one channel completely inhibits the other: the contribution of both channels might be reduced so that the result resembles the response to the stronger channel alone. Either way, it suggests a mechanism involving synaptic inhibition between glomeruli. Our data are probably not explained by lateral inhibition in the first relay of the olfactory system (the antennal lobe), because lateral inhibition in the antennal lobe is not measurably recruited by activating one or two glomeruli; it requires co-activating a larger number of glomeruli, and it appears to be a gain control mechanism that is mainly recruited at higher stimulus intensities (Olsen et al., 2010; Root et al., 2011). Instead, the max-pooling operations we have observed are more likely implemented in higher brain regions. Indeed, these regions contain circuit elements that can mediate antagonistic interactions between odor stimuli (Fişek and Wilson, 2014; Jefferis et al., 2007; Lai et al., 2008; Lewis et al., 2015; Liang et al., 2013; Owald et al., 2015; Parnas et al., 2013; Strutz et al., 2014).

Our data could be explained by inhibition among individual glomeruli, or by inhibition among groups of glomeruli. Consider the four glomeruli in Figure 5: we can account for these data with a network in which specific pairs of glomeruli inhibit each other. Alternatively, we can draw a network in which specific groups of glomeruli converge onto downstream targets, and these targets then inhibit each other (Figure S8). These network diagrams imply testable predictions about the wiring of higher olfactory brain regions. Specifically, we predict that certain pairs of glomeruli are likely to send excitatory projections to common targets (i.e., the green pairs in Figure 6). Other pairs of glomeruli reduce each other's potency (the magenta pairs in Figure 6), and so we predict that inhibition occurs preferentially between these glomeruli, or between groups of glomeruli that contain these pairs (Figure S8).

Of course, at the circuit level, convergence and mutual inhibition are not mutually exclusive. Indeed, DM1 and DM2 are known to send convergent excitation to one lateral horn neuron subtype (Fişek and Wilson, 2014), but we find that the behavioral interaction between these glomeruli is max pooling rather than summation (Figure 5D). This behavioral result suggests there are inhibitory circuit interactions between these glomeruli that can dominate over the effects of convergence.

What Combinations of Glomeruli Mean to the Organism

Interestingly, we found that all attractive glomeruli recruited the same behavioral program (Figure 8). Some glomeruli recruited this behavioral program with a low frequency (e.g., glomerulus DM2), and others with a higher frequency (e.g., glomerulus DM1). When we co-stimulated a second glomerulus, we found some cases in which attraction increased, but other cases in which the level of attraction remained the same. Why should this be so, from the organism's perspective?

It is likely that the behavior of the flies we studied was shaped by multiple competing factors in addition to the fictive odor. Indeed, we never saw a single fly choose an attractive fictive odor in 100% of trials, even when the stimulus intensity was so high as to make ensemble ORN spiking responses unambiguous (Figure 1). Pursuing an odor requires the fly to forgo other opportunities—e.g., the opportunity to explore the environment. The percentage of instances in which the fly chooses the odor should ideally reflect the expected value of the odor. When two equally attractive glomeruli are stimulated simultaneously, the expected value of choosing to pursue the odor may not double, because the two glomerular signals may represent partly redundant evidence of future value. We might view the brain's task as computing the probability distribution of expected value, marginalized over many natural odor sources, given the observed pattern of ORN firing rates (Beck et al., 2011). From this perspective, the pattern of glomerular interactions revealed by our data may represent a heuristic estimate of conditional probabilities of expected value—an estimate learned during the fly's lifetime, or else shaped by natural selection over evolutionary time.

EXPERIMENTAL PROCEDURES

Fly Care and Genotypes
Flies were hemizygous $NorpA^7$ males 6–8 days old. The $NorpA^7$ mutation was used to eliminate positive phototaxis in control flies (Figure S2). Flies were raised on food supplemented with all-*trans* retinal and were deprived of all food for 12 hr before testing. Genotypes used in each figure are listed in Table S1. Details of all Gal4 lines are listed in Table S2. Whenever possible, we performed experiments with two different Gal4 lines targeting the same ORN type, and results were generally similar in both cases (Figure S3). See Supplemental Experimental Procedures for details on fly genotypes, fly care, and genetic controls.

Electrophysiology
We used standard methods to perform extracellular recordings from ORNs. All data from these experiments are displayed in Figure S1. A few ORN types in our study are not accessible to electrophysiology, but all these ORN types did elicit behavioral responses (Table S2). See Supplemental Experimental Procedures for details on electrophysiological recordings, spike sorting, and spike rate analysis.

Design and Calibration of Light Stimuli
Light stimuli were generated by blue (445 nm, 500 mW) and red (635 nm, 550 mW) pulsed diode lasers. During each stimulus epoch, a fly was illuminated by a brief pulse every 50 ms. Pulse width of both beams was modulated to vary the fictive odor intensity while maintaining a total intensity at all locations of 1.5 mW/mm². See Supplemental Experimental Procedures for details on stimulus calibration.

Behavior Chambers and Tracking
Each fly was isolated in its own 50 × 5 × 1.2-mm chamber (Claridge-Chang et al., 2009; Parnas et al., 2013). Air (35 cm/s) entered at the ends of the chamber and exited through ports in the center. Real-time image analysis was used to steer a pair of mirrors that re-positioned the laser beams on each fly as it moved. The lasers were positioned sequentially onto each of eight simultaneously tracked flies (in separate chambers). The stimulus epoch was 30 s and the inter-stimulus interval was 3 min. The intensity of the blue stimulus, and whether it was on the left or right side of the chamber, was varied pseudorandomly. See Supplemental Experimental Procedures for details on chambers, tracking, and positive controls with real odor.

Preference Index
The Preference Index (PI) was calculated following Claridge-Chang et al. (2009) and Parnas et al. (2013) based on exits from the "choice zone" (Figure 2A):

$$PI = (\text{exits toward blue} - \text{exits toward red})/(\text{exits toward blue} + \text{exits toward red}).$$

See Supplemental Experimental Procedures for details.

Statistics
Unless otherwise noted, all error bars denote 95% confidence intervals calculated by bootstrap resampling. Bootstrap tests were used to assess differences between genotypes, and also differences between models and data. See Supplemental Experimental Procedures for details on the Reliability metric (Figure 8) as well as other statistics.

Principal Component Analysis
The input to principal component analysis (PCA) in Figure 8 was the matrix containing measurements of the 12 behavioral variables measured over all 8 light intensities in 13 genotypes, where each measurement is a mean over all flies of a given genotype tested with a particular light intensity, and each mean value is duplicated in the matrix so it is weighted in proportion to the number of flies contributing to that mean value. We term this "Signal PCA." See Supplemental Experimental Procedures for details.

Code Availability
Code for spike sorting, video tracking, Signal PCA, calculation of bivariate confidence intervals, and behavioral analysis is available for download at http://wilson.med.harvard.edu/BellWilson2016Code.html.

SUPPLEMENTAL INFORMATION

Supplemental Information includes Supplemental Experimental Procedures, eight figures, and three tables and can be found with this article online at http://dx.doi.org/10.1016/j.neuron.2016.06.011.

AUTHOR CONTRIBUTIONS

J.S.B. and R.I.W. designed all experiments. J.S.B. performed all experiments and data analysis. J.S.B. and R.I.W. wrote the manuscript.

REFERENCES

Ai, M., Min, S., Grosjean, Y., Leblanc, C., Bell, R., Benton, R., and Suh, G.S. (2010). Acid sensing by the Drosophila olfactory system. Nature *468*, 691–695.

Baker, T.C. (2008). Balanced olfactory antagonism as a concept for understanding evolutionary shifts in moth sex pheromone blends. J. Chem. Ecol. *34*, 971–981.

Beck, J.M., Latham, P.E., and Pouget, A. (2011). Marginalization in neural circuits with divisive normalization. J. Neurosci. *31*, 15310–15319.

Bell, W.J., and Kramer, E. (1979). Search and anemotactic orientation of cockroaches. J. Insect Physiol. 25, 631–640.

Bellmann, D., Richardt, A., Freyberger, R., Nuwal, N., Schwärzel, M., Fiala, A., and Störtkuhl, K.F. (2010). Optogenetically induced olfactory stimulation in Drosophila larvae reveals the neuronal basis of odor-aversion behavior. Front. Behav. Neurosci. 4, 27.

Bhandawat, V., Maimon, G., Dickinson, M.H., and Wilson, R.I. (2010). Olfactory modulation of flight in Drosophila is sensitive, selective and rapid. J. Exp. Biol. 213, 3625–3635.

Budick, S.A., and Dickinson, M.H. (2006). Free-flight responses of Drosophila melanogaster to attractive odors. J. Exp. Biol. 209, 3001–3017.

Caron, S.J., Ruta, V., Abbott, L.F., and Axel, R. (2013). Random convergence of olfactory inputs in the Drosophila mushroom body. Nature 497, 113–117.

Claridge-Chang, A., Roorda, R.D., Vrontou, E., Sjulson, L., Li, H., Hirsh, J., and Miesenböck, G. (2009). Writing memories with light-addressable reinforcement circuitry. Cell 139, 405–415.

Couto, A., Alenius, M., and Dickson, B.J. (2005). Molecular, anatomical, and functional organization of the Drosophila olfactory system. Curr. Biol. 15, 1535–1547.

de Bruyne, M., Clyne, P.J., and Carlson, J.R. (1999). Odor coding in a model olfactory organ: the Drosophila maxillary palp. J. Neurosci. 19, 4520–4532.

de Bruyne, M., Foster, K., and Carlson, J.R. (2001). Odor coding in the Drosophila antenna. Neuron 30, 537–552.

Devaud, J.M., Acebes, A., and Ferrús, A. (2001). Odor exposure causes central adaptation and morphological changes in selected olfactory glomeruli in Drosophila. J. Neurosci. 21, 6274–6282.

Dewan, A., Pacifico, R., Zhan, R., Rinberg, D., and Bozza, T. (2013). Non-redundant coding of aversive odours in the main olfactory pathway. Nature 497, 486–489.

Duchamp-Viret, P., Duchamp, A., and Chaput, M.A. (2003). Single olfactory sensory neurons simultaneously integrate the components of an odour mixture. Eur. J. Neurosci. 18, 2690–2696.

Duistermars, B.J., Chow, D.M., and Frye, M.A. (2009). Flies require bilateral sensory input to track odor gradients in flight. Curr. Biol. 19, 1301–1307.

Faucher, C., Forstreuter, M., Hilker, M., and de Bruyne, M. (2006). Behavioral responses of Drosophila to biogenic levels of carbon dioxide depend on life-stage, sex and olfactory context. J. Exp. Biol. 209, 2739–2748.

Fişek, M., and Wilson, R.I. (2014). Stereotyped connectivity and computations in higher-order olfactory neurons. Nat. Neurosci. 17, 280–288.

Fishilevich, E., and Vosshall, L.B. (2005). Genetic and functional subdivision of the Drosophila antennal lobe. Curr. Biol. 15, 1548–1553.

Gao, X.J., Clandinin, T.R., and Luo, L. (2015). Extremely sparse olfactory inputs are sufficient to mediate innate aversion in Drosophila. PLoS ONE 10, e0125986.

Gaudry, Q., Hong, E.J., Kain, J., de Bivort, B., and Wilson, R.I. (2013). Asymmetric neurotransmitter release enables rapid odour lateralization in Drosophila. Nature 493, 424–428.

Gruntman, E., and Turner, G.C. (2013). Integration of the olfactory code across dendritic claws of single mushroom body neurons. Nat. Neurosci. 16, 1821–1829.

Haddad, R., Weiss, T., Khan, R., Nadler, B., Mandairon, N., Bensafi, M., Schneidman, E., and Sobel, N. (2010). Global features of neural activity in the olfactory system form a parallel code that predicts olfactory behavior and perception. J. Neurosci. 30, 9017–9026.

Hallem, E.A., and Carlson, J.R. (2006). Coding of odors by a receptor repertoire. Cell 125, 143–160.

Hernandez-Nunez, L., Belina, J., Klein, M., Si, G., Claus, L., Carlson, J.R., and Samuel, A.D. (2015). Reverse-correlation analysis of navigation dynamics in Drosophila larva using optogenetics. eLife 4, e06225.

Jefferis, G.S., Potter, C.J., Chan, A.M., Marin, E.C., Rohlfing, T., Maurer, C.R., Jr., and Luo, L. (2007). Comprehensive maps of Drosophila higher olfactory centers: spatially segregated fruit and pheromone representation. Cell 128, 1187–1203.

Jinks, A., and Laing, D.G. (2001). The analysis of odor mixtures by humans: evidence for a configurational process. Physiol. Behav. 72, 51–63.

Jung, S.H., Hueston, C., and Bhandawat, V. (2015). Odor-identity dependent motor programs underlie behavioral responses to odors. eLife 4, 4.

Kain, P., Boyle, S.M., Tharadra, S.K., Guda, T., Pham, C., Dahanukar, A., and Ray, A. (2013). Odour receptors and neurons for DEET and new insect repellents. Nature 502, 507–512.

Kazama, H., and Wilson, R.I. (2008). Homeostatic matching and nonlinear amplification at identified central synapses. Neuron 58, 401–413.

Keller, A., Zhuang, H., Chi, Q., Vosshall, L.B., and Matsunami, H. (2007). Genetic variation in a human odorant receptor alters odour perception. Nature 449, 468–472.

Kennedy, J.S. (1977). Olfactory responses to distant plants and other odor sources. In Chemical Control of Insect Behavior: Theory and Application, H.H. Shorey and J.J. McKelvey, Jr., eds. (Wiley), pp. 67–91.

Kennedy, J.S. (1978). The concepts of olfactory 'arrestrnent' and 'attraction'. Physiol. Entomol. 3, 91–98.

Knaden, M., Strutz, A., Ahsan, J., Sachse, S., and Hansson, B.S. (2012). Spatial representation of odorant valence in an insect brain. Cell Rep. 1, 392–399.

Kreher, S.A., Mathew, D., Kim, J., and Carlson, J.R. (2008). Translation of sensory input into behavioral output via an olfactory system. Neuron 59, 110–124.

Kurtovic, A., Widmer, A., and Dickson, B.J. (2007). A single class of olfactory neurons mediates behavioural responses to a Drosophila sex pheromone. Nature 446, 542–546.

Lai, S.L., Awasaki, T., Ito, K., and Lee, T. (2008). Clonal analysis of Drosophila antennal lobe neurons: diverse neuronal architectures in the lateral neuroblast lineage. Development 135, 2883–2893.

Larsson, M.C., Domingos, A.I., Jones, W.D., Chiappe, M.E., Amrein, H., and Vosshall, L.B. (2004). Or83b encodes a broadly expressed odorant receptor essential for Drosophila olfaction. Neuron 43, 703–714.

Lewis, L.P., Siju, K.P., Aso, Y., Friedrich, A.B., Bulteel, A.J., Rubin, G.M., and Grunwald Kadow, I.C. (2015). A higher brain circuit for immediate integration of conflicting sensory information in Drosophila. Curr. Biol. 25, 2203–2214.

Liang, L., Li, Y., Potter, C.J., Yizhar, O., Deisseroth, K., Tsien, R.W., and Luo, L. (2013). GABAergic projection neurons route selective olfactory inputs to specific higher-order neurons. Neuron 79, 917–931.

Mathew, D., Martelli, C., Kelley-Swift, E., Brusalis, C., Gershow, M., Samuel, A.D., Emonet, T., and Carlson, J.R. (2013). Functional diversity among sensory receptors in a Drosophila olfactory circuit. Proc. Natl. Acad. Sci. USA 110, E2134–E2143.

Olsen, S.R., Bhandawat, V., and Wilson, R.I. (2010). Divisive normalization in olfactory population codes. Neuron 66, 287–299.

Owald, D., Felsenberg, J., Talbot, C.B., Das, G., Perisse, E., Huetteroth, W., and Waddell, S. (2015). Activity of defined mushroom body output neurons underlies learned olfactory behavior in Drosophila. Neuron 86, 417–427.

Parker, A.J., and Newsome, W.T. (1998). Sense and the single neuron: probing the physiology of perception. Annu. Rev. Neurosci. 21, 227–277.

Parnas, M., Lin, A.C., Huetteroth, W., and Miesenböck, G. (2013). Odor discrimination in Drosophila: from neural population codes to behavior. Neuron 79, 932–944.

Root, C.M., Ko, K.I., Jafari, A., and Wang, J.W. (2011). Presynaptic facilitation by neuropeptide signaling mediates odor-driven food search. Cell 145, 133–144.

Sachse, S., Rueckert, E., Keller, A., Okada, R., Tanaka, N.K., Ito, K., and Vosshall, L.B. (2007). Activity-dependent plasticity in an olfactory circuit. Neuron 56, 838–850.

Semmelhack, J.L., and Wang, J.W. (2009). Select Drosophila glomeruli mediate innate olfactory attraction and aversion. Nature 459, 218–223.

Silbering, A.F., Rytz, R., Grosjean, Y., Abuin, L., Ramdya, P., Jefferis, G.S., and Benton, R. (2011). Complementary function and integrated wiring of the evolutionarily distinct Drosophila olfactory subsystems. J. Neurosci. *31*, 13357–13375.

Smear, M., Resulaj, A., Zhang, J., Bozza, T., and Rinberg, D. (2013). Multiple perceptible signals from a single olfactory glomerulus. Nat. Neurosci. *16*, 1687–1691.

Steck, K., Veit, D., Grandy, R., Badia, S.B., Mathews, Z., Verschure, P., Hansson, B.S., and Knaden, M. (2012). A high-throughput behavioral paradigm for Drosophila olfaction - The Flywalk. Sci. Rep. *2*, 361.

Stensmyr, M.C., Dweck, H.K., Farhan, A., Ibba, I., Strutz, A., Mukunda, L., Linz, J., Grabe, V., Steck, K., Lavista-Llanos, S., et al. (2012). A conserved dedicated olfactory circuit for detecting harmful microbes in Drosophila. Cell *151*, 1345–1357.

Strutz, A., Soelter, J., Baschwitz, A., Farhan, A., Grabe, V., Rybak, J., Knaden, M., Schmuker, M., Hansson, B.S., and Sachse, S. (2014). Decoding odor quality and intensity in the Drosophila brain. eLife *3*, e04147.

Su, C.Y., Menuz, K., and Carlson, J.R. (2009). Olfactory perception: receptors, cells, and circuits. Cell *139*, 45–59.

Suh, G.S., Wong, A.M., Hergarden, A.C., Wang, J.W., Simon, A.F., Benzer, S., Axel, R., and Anderson, D.J. (2004). A single population of olfactory sensory neurons mediates an innate avoidance behaviour in Drosophila. Nature *431*, 854–859.

Suh, G.S., Ben-Tabou de Leon, S., Tanimoto, H., Fiala, A., Benzer, S., and Anderson, D.J. (2007). Light activation of an innate olfactory avoidance response in Drosophila. Curr. Biol. *17*, 905–908.

Tanaka, N.K., Awasaki, T., Shimada, T., and Ito, K. (2004). Integration of chemosensory pathways in the Drosophila second-order olfactory centers. Curr. Biol. *14*, 449–457.

Thoma, M., Hansson, B.S., and Knaden, M. (2014). Compound valence is conserved in binary odor mixtures in Drosophila melanogaster. J. Exp. Biol. *217*, 3645–3655.

Turner, S.L., and Ray, A. (2009). Modification of CO2 avoidance behaviour in Drosophila by inhibitory odorants. Nature *461*, 277–281.

van Breugel, F., and Dickinson, M.H. (2014). Plume-tracking behavior of flying Drosophila emerges from a set of distinct sensory-motor reflexes. Curr. Biol. *24*, 274–286.